Indirect radiative forcing of climate change through ozone effects on the land-carbon sink

S. Sitch[1], P. M. Cox[3], W. J. Collins[4] & C. Huntingford[2]

The evolution of the Earth's climate over the twenty-first century depends on the rate at which anthropogenic carbon dioxide emissions are removed from the atmosphere by the ocean and land carbon cycles[1]. Coupled climate–carbon cycle models suggest that global warming will act to limit the land-carbon sink[2], but these first generation models neglected the impacts of changing atmospheric chemistry. Emissions associated with fossil fuel and biomass burning have acted to approximately double the global mean tropospheric ozone concentration[3], and further increases are expected over the twenty-first century[4]. Tropospheric ozone is known to damage plants, reducing plant primary productivity and crop yields[5], yet increasing atmospheric carbon dioxide concentrations are thought to stimulate plant primary productivity[6]. Increased carbon dioxide and ozone levels can both lead to stomatal closure, which reduces the uptake of either gas, and in turn limits the damaging effect of ozone and the carbon dioxide fertilization of photosynthesis[6]. Here we estimate the impact of projected changes in ozone levels on the land-carbon sink, using a global land carbon cycle model modified to include the effect of ozone deposition on photosynthesis and to account for interactions between ozone and carbon dioxide through stomatal closure[7]. For a range of sensitivity parameters based on manipulative field experiments, we find a significant suppression of the global land-carbon sink as increases in ozone concentrations affect plant productivity. In consequence, more carbon dioxide accumulates in the atmosphere. We suggest that the resulting indirect radiative forcing by ozone effects on plants could contribute more to global warming than the direct radiative forcing due to tropospheric ozone increases.

Tropospheric ozone (O_3) is a naturally occurring greenhouse gas formed as a product of photochemical reactions with precursors: NO_x, CH_4, CO and volatile organic compounds. Over the industrial period, anthropogenic precursor emissions from fossil fuel and biomass burning have led to elevated ambient ozone concentrations ($[O_3]$) over a large portion of the Earth's surface (Fig. 1), resulting in a direct radiative forcing of climate change of $+0.35^{-0.1}_{+0.3}\,\mathrm{W\,m}^{-2}$ (ref. 8). Many regions of the globe are already experiencing near-surface ozone levels greater than 40 parts per billion (40 p.p.b.)—levels that may cause visible leaf injury and plant damage, and reduction in crop yields[5], with associated economic costs of several billion dollars per annum in each of the US, EU and East Asia[5,9].

Concentrations of atmospheric CO_2 and near surface ozone are expected to increase significantly through the next century, although the magnitude of the increases depends on the particular emission scenario chosen. Here we use the SRES A2 scenario for comparability with recent atmospheric chemistry simulations[10], but our overall conclusion is insensitive to this choice. Under SRES A2, mean monthly 24-h ozone concentrations by 2100 are projected to be above 40 p.p.b. over almost all regions, and to exceed 70 p.p.b. over western and central Eurasia, eastern and western North America, Brazil, central and southwestern Africa, and East Asia, during the Northern Hemisphere summer (Fig. 1).

Ozone causes cellular damage inside leaves that adversely affects plant production, reduces photosynthetic rates and requires increased resource allocation to detoxify and repair leaves[5]. There have been few global modelling studies of the impact of tropospheric ozone on plant production and global land-carbon storage[11], and no study has estimated the indirect radiative forcing of tropospheric ozone through feedbacks on the global carbon cycle. Here, we are concerned with the possible impacts of future tropospheric ozone on global-scale plant primary production, land-carbon storage, and its implications for twenty-first-century climate change.

Future elevated $[CO_2]$ may itself lead to reductions in stomatal conductance[12] at levels that act to alleviate future O_3 plant damage. Hence, future O_3 effects on plants are defined by the interplay of ambient $[O_3]$, $[CO_2]$ and climate change on stomatal conductance and plant production, with important ramifications for global land-carbon and hydrological cycles[7,11]. Free air CO_2 enrichment (FACE) experiments and other ambient air experiments indicate a nonlinear interaction between plant responses to CO_2 and O_3 (refs 6, 13–15). To account for these interactions, we use a flux-gradient approach to modelling ozone damage[16], rather than the more usual empirical approach based on the accumulated ozone exposure above 40 p.p.b. (ref. 11). We modify the MOSES-TRIFFID land-surface scheme[17], assuming a suppression of net leaf photosynthesis by ozone that varies proportionally to the ozone flux through stomata above a specified critical ozone deposition flux. Our scheme includes an empirical relationship between stomatal conductance and photosynthesis[18], and through this mechanism the direct effect of O_3 deposition on photosynthesis also leads to a reduction in stomatal conductance. As the O_3 flux itself depends on the stomatal conductance, which in turn depends upon the net rate of photosynthesis[18], the model requires a consistent solution for the net photosynthesis, stomatal conductance and the ozone deposition flux (see Methods).

This more mechanistic approach to modelling ozone effects on photosynthesis accounts for the complex interaction between CO_2 and O_3 effects. Increases in the concentration of either gas lead to stomatal closure, which may limit the uptake of the other gas. Thus the model can be used to assess the extent to which CO_2-induced stomatal closure[7] will protect plants against the potentially damaging impacts of increases in near-surface O_3, or conversely the extent to which O_3 increases will limit CO_2-fertilization of photosynthesis and thereby reduce the ability of ecosystems to mitigate global warming. In this study, we focus on the interplay between future projections of O_3 and CO_2 on plant physiology and the land carbon cycle, but acknowledge the importance of the additional and uncertain

[1]Met Office, Hadley Centre for Climate Prediction and Research (JCHMR), Maclean Building, [2]Centre for Ecology and Hydrology Wallingford, Maclean Building, Wallingford, OX10 8BB, UK. [3]School of Engineering, Computer Science and Mathematics, University of Exeter, Exeter, ES4 4QF, UK. [4]Met Office, Hadley Centre for Climate Prediction and Research, Fitzroy Road, Exeter, EX1 3PB, UK.
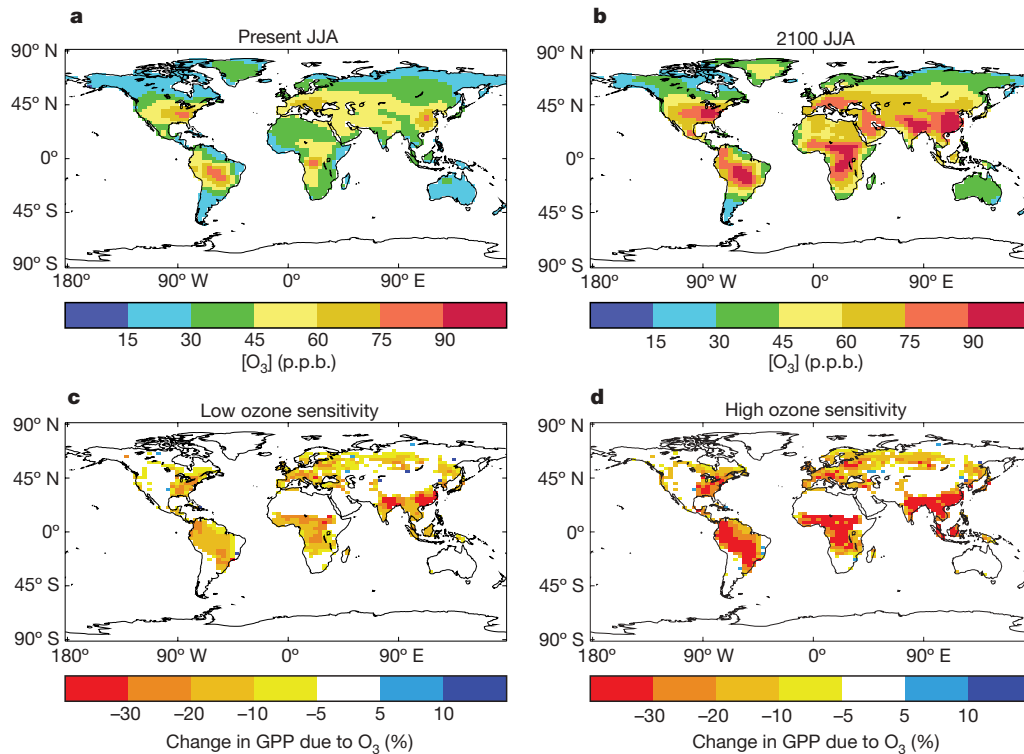
Figure 1 | Temporal changes of modelled ozone concentrations and gross primary productivity. a, b, Modelled diurnal (24-h) mean surface $[O_3]$ in p.p.b. averaged over June, July and August (JJA) for the present day (**a**) and the year 2100 under the SRES A2 emissions scenario (**b**). **c, d,** Simulated percentage change in gross primary productivity (GPP) between 1901 and 2100 due to O_3 effects at fixed pre-industrial atmospheric $[CO_2]$ for 'low' (**c**) and 'high' (**d**) ozone plant sensitivity.

interactions between a changing climate, stomatal conductance, ozone uptake and plant productivity.

We use spatially explicit $[O_3]$ fields derived from the STOCHEM model[19] to drive the modified MOSES-TRIFFID land-surface scheme[17] offline. Two model versions are applied, with 'high' and 'low' plant ozone sensitivity based on observations[16,20]. For model evaluation against global carbon cycle budgets, simulations are conducted for the period 1901–2002, using a monthly observational data set of the twentieth-century climate[21], changing monthly fields of diurnal mean $[O_3]$ and prescribed annual fields of global atmospheric $[CO_2]$. As a further model evaluation, a second set of simulations replicates the Aspen FACE experiment[6,13] and the free-air O_3 fumigation experiment at a Swiss grassland site[14]. The Aspen FACE experiment investigates the response of maturing aspen stands across a wide range of O_3 sensitivity in five aspen clones. Plots were planted in 1997 and exposed for seven years to combinations of ambient and elevated concentrations of $[CO_2]$ and $[O_3]$, with elevated $[CO_2]$ at 560 p.p.m.v., and elevated $[O_3]$ at 1.5 times ambient levels. In the grassland experiments, plots are exposed for 5 years to ambient and elevated $[O_3]$ at 1.5 times ambient levels. Our simulations broadly agree with the results from these free air enrichment Swiss grassland and aspen experiments[6,13,14] (see Supplementary Fig. 3), and an ozone risk mapping for North America derived from the Aspen FACE results[15].

A third set of factorial simulations is conducted from 1901 to 2100 with changing fields of monthly near-surface tropospheric ozone and atmospheric CO_2 concentrations consistent with the A2 SRES scenario. A fixed mean monthly pre-industrial climate is prescribed in these runs, in order to focus on the interaction between direct CO_2 and O_3 effects on plant physiology. For each of the 'high' and 'low' ozone plant sensitivity parameterizations, three simulations are conducted with combinations of fixed pre-industrial and prescribed changing fields of $[O_3]$ and global atmospheric $[CO_2]$.

Over the 1990s, global mean land–atmosphere fluxes of $-1.34\,\mathrm{Pg\,C\,yr^{-1}}$ and $-1.74\,\mathrm{Pg\,C\,yr^{-1}}$ are simulated for the 'high'

and 'low' plant O_3 sensitivity models, respectively, both within the IPCC range[22] of $-4.3\,\mathrm{Pg\,C\,yr^{-1}}$ to $-0.9\,\mathrm{Pg\,C\,yr^{-1}}$ with a mean of $-2.6\,\mathrm{Pg\,C\,yr^{-1}}$ (Supplementary Table 2). Figure 1 shows the impact of O_3 increases on the pattern of gross primary productivity (GPP) by 2100. The lower panels show the percentage change in GPP due to O_3 in the model runs with fixed pre-industrial CO_2. Over the period 1901–2100, global GPP is projected to decrease by 14–23% owing to plant ozone damage (Supplementary Table 3), with regional reductions above 30% (Fig. 1). Large reductions in GPP and land-carbon storage are projected over North America, Europe, China and India, regions with the highest levels of human appropriation of primary productivity[23], and in tropical ecosystems, raising important issues concerning the vulnerability of regional ecosystem services (for example, food security, forest productivity and carbon sequestration)[24] to changes in air quality.

The combined effect of elevated future $[CO_2]$ and $[O_3]$ on plant physiology is an increase in global GPP and net land carbon uptake (Table 1). However, the enhancement in global GPP at 2100, by the

Table 1 | Simulated changes in the global land carbon cycle due to O_3 and CO_2 increases

Model	GPP (Pg C yr⁻¹)	Veg. C (Pg C)	Soil C (Pg C)	Land C (Pg C)
'High' plant O_3 sensitivity				
Value in 1901	112.7	461.8	1,110.8	1,572.6
Δ Value (2100–1901)				
Δ[CO₂], fixed [O₃]	88.4	235.0	621.7	856.7
Fixed [CO₂], Δ[O₃]	−26.4	−89.1	−173.4	−262.5
Δ[CO₂] and Δ[O₃]	58.4	184.8	432.7	617.5
'Low' plant O_3 sensitivity				
Value in 1901	116.6	488.2	1,130.2	1,618.4
Δ Value (2100–1901)				
Δ[CO₂], fixed [O₃]	86.9	217.5	618.3	835.8
Fixed [CO₂], Δ[O₃]	−16.1	−31.9	−111.3	−143.2
Δ[CO₂] and Δ[O₃]	71.3	201.9	513.8	715.6

Shown are changes (Δ) in global gross primary production (GPP) and global carbon stocks in vegetation (Veg.) and soils between 1901 and 2100.

physiological effects of elevated [CO_2], is reduced by between 15.6 Pg C yr^{-1} and 30.0 Pg C yr^{-1}, for the 'low' and 'high' plant ozone sensitivity, respectively, when concurrent ozone impacts on vegetation are also considered. This process is not accounted for in the current generation of climate–carbon cycle models[2].

A novel aspect of adopting a flux-gradient approach to modelling leaf gas exchange of both O_3 and CO_2 is that it enables investigation not only of the individual effects of O_3 and CO_2 acting in isolation on plant physiology, but also of their interaction.

Elevated CO_2 provides some protection against O_3 damage, by way of reductions in stomatal conductance and a concomitant decrease in plant ozone uptake. We diagnose this protection by comparing the O_3-induced percentage reductions in GPP at 2100 from the runs with and without prescribed CO_2 increases (Supplementary Fig. 1, right-hand panels). CO_2 fertilization is projected to increase GPP significantly, so while the absolute effect of O_3 on GPP is greater under increasing rather than constant CO_2, the fractional change is much smaller. CO_2-induced stomatal closure is found to offset O_3-suppression of GPP by over one-third, such that GPP by 2100 is 8–15% lower due to O_3 exposure, rather than 14–23% lower in the absence of CO_2 increases (see Supplementary Table 3). This

Figure 2 | Temporal changes in land carbon storage and radiative forcing due to ozone. a, b, Simulated change in land carbon storage (**a**) and indirect radiative forcing due to O_3 increases alone (**b**), for 'high' (red) and 'low' (blue) plant sensitivities to ozone. These results are diagnosed from model simulations using a fixed pre-industrial CO_2 concentration. For comparison, estimates of the direct radiative forcing due to O_3 increases are shown by the bars in **b**. Present-day direct radiative forcing comes from the STOCHEM-HadGEM1 tropospheric ozone fields (black square), with the bars showing the range of estimates from other atmospheric chemistry models[3]. Estimates of future direct radiative forcing due to O_3 relative to 1900 are derived from the IPCC TAR (0xComp) models[4]. These values represent the radiative forcing due to changes in tropospheric ozone over the twenty-first century. They are added to the IPCC mean radiative forcing of 0.38 W m^{-2} (representing the period between pre-industrial to 2000)[28] from which a global mean radiative forcing value of 0.05 W m^{-2} (between 1850 and 1900) (ref. 27) is subtracted. The black triangle denotes the model mean, and the bars show the range across the models.

nonlinear interaction between the relative effects of CO_2 and O_3 increases is typically ignored in modelling approaches based on the cumulative O_3 exposure rather than uptake by leaves.

There are large potential impacts of elevated future [O_3] on the ability of many ecosystems to sequester carbon (Table 1). Over the period 1900–2100, changes in [O_3] with all other forcings fixed are projected to reduce land-carbon storage accumulation by between 143 Pg C and 263 Pg C (Fig. 2a, Supplementary Fig. 4). This is equivalent to a reduction of between 17% and 31% in the projected land uptake associated with the plant physiological response to CO_2 increase alone. However, there are significant uncertainties in the response of different plant species to O_3, especially for tropical ecosystems, and in the scaling up of open top chamber results[25] (for example, uncertainties associated with chamber effects), both warranting further research. In our present study, ozone response data for European and North American species have been extrapolated to represent all global vegetation types.

Suppression of the land-carbon sink results in additional anthropogenic CO_2 emissions accumulating in the atmosphere, and therefore an indirect radiative forcing of climate change by O_3 effects on the terrestrial biosphere. The indirect radiative forcing due to O_3 is diagnosed for comparison to the direct forcing due to tropospheric O_3 (Fig. 2b), assuming 50% of the extra CO_2 from the land is sequestered by the oceans[26]. The indirect forcing by 2100 is estimated at 0.62 W m^{-2} and 1.09 W m^{-2} for the 'low' and 'high' plant ozone sensitivity runs, respectively, which compares with a mean direct radiative forcing from 11 atmospheric chemistry models of 0.89 W m^{-2} (refs 3, 4, 27, 28). Although the absolute values of radiative forcing are dependent on our choice of emissions scenario, the relative importance of direct and indirect radiative forcing is much less sensitive to the uncertainty in emissions. As such, these results suggest that ozone effects on vegetation could double the effective radiative forcing due to increases in tropospheric ozone, significantly increasing the importance of changes in atmospheric chemistry as a driver of twenty-first-century climate change.
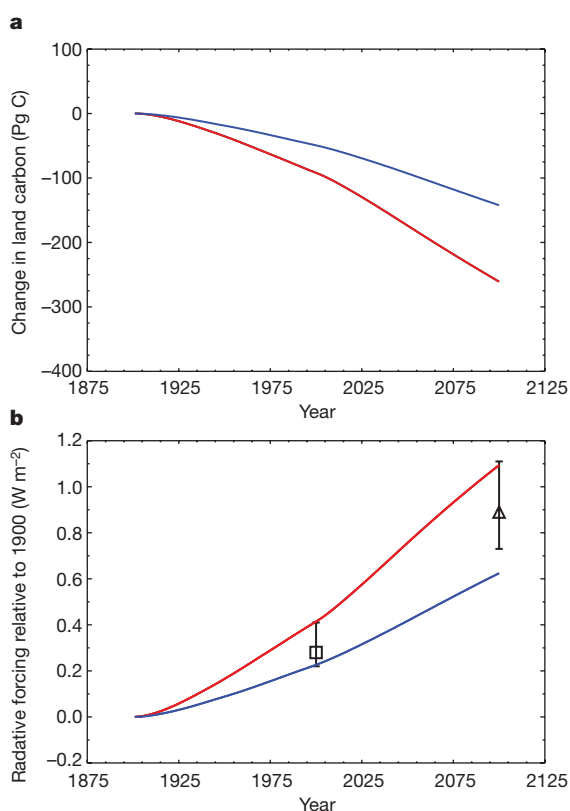
METHODS SUMMARY

Our approach is to modify net photosynthesis by a factor that accounts for plant ozone uptake and plant-specific sensitivities to ozone uptake. Ozone uptake is dependent on stomatal conductance, itself dependent on the photosynthetic rate in MOSES. The resulting equations are solved analytically to obtain a consistent solution for ozone uptake, stomatal conductance and ozone-modified net photosynthesis. Data from field observation[16,20] are used to calibrate plant-ozone effects for the five plant functional types (PFTs) described by MOSES. A 'high' and 'low' parameterization is chosen for each PFT to represent uncertainty in the responses of different plant species to ozone deposition.

The Met Office's lagrangian tropospheric chemistry model STOCHEM[19] was used to generate monthly mean surface ozone concentrations for the present day (2000) using emissions from the IIASA CLE scenario[28], and for the future (2100) using emissions from the SRES A2 scenario.

As described in ref. 7, this study uses the 0.5° resolution observational data set from the Climate Research Unit, which contains monthly temperature (mean and diurnal range), humidity, cloud cover and precipitation (amount and daily frequency). Empirical formulations are used to derive shortwave and longwave radiation from the Climate Research Unit data set. All monthly forcing data are regridded onto the HadCM3 2.5° × 3.75° grid and disaggregated to hourly data.

Full Methods and any associated references are available in the online version of the paper at www.nature.com/nature.

1. Cox, P. M., Betts, R. A., Jones, C. D., Spall, S. A. & Totterdell, I. J. Acceleration of global warming due to carbon-cycle feedbacks in a coupled climate model. *Nature* **408**, 184–187 (2000).
2. Friedlingstein, P. *et al.* Climate-carbon cycle feedback analysis: results from the C4MIP model intercomparison. *J. Clim.* **19**, 3337–3353 (2006).
3. Gauss, M. *et al.* Radiative forcing since preindustrial times due to ozone change in the troposphere and the lower stratosphere. *Atmos. Chem. Phys.* **6**, 575–599 (2006).

4. Gauss, M. *et al.* Radiative forcing in the 21st century due to ozone changes in the troposphere and the lower stratosphere. *J. Geophys. Res.* **108**, 4292, doi:10.1029/2002JD002624 (2003).
5. Ashmore, M. R. Assessing the future global impacts of ozone on vegetation. *Plant Cell Environ.* **28**, 949–964 (2005).
6. Karnosky, D. F. *et al.* Tropospheric O_3 modulates responses of temperate hardwood forests to elevated CO_2: a synthesis of molecular to ecosystem results from the Aspen FACE project. *Funct. Ecol.* **17**, 289–304 (2003).
7. Gedney, N. *et al.* Detection of a direct carbon dioxide effect in continental river runoff records. *Nature* **439**, 835–838 (2006).
8. Forster, P. *et al.* in *Climate Change 2007: The Physical Science Basis* (eds Solomon, S. *et al.*) 129–234 (Cambridge Univ. Press, Cambridge, UK, 2007).
9. Wang, X. & Mauzerall, D. L. Characterizing distributions of surface ozone and its impact on grain production in China, Japan and South Korea: 1900 and 2020. *Atmos. Environ.* **38**, 4383–4402 (2004).
10. Prather, M. *et al.* in *Climate Change 2001: The Scientific Basis* (eds Houghton, J. T. *et al.*) 239–287 (Cambridge Univ. Press, Cambridge, UK, 2001).
11. Felzer, B. S. *et al.* Future effects of ozone on carbon sequestration and climate change policy using a global biogeochemical model. *Clim. Change* **73**, 345–373, doi:10.1007/s10584-005-6776-4 (2005).
12. Field, C., Jackson, R. & Mooney, H. Stomatal responses to increased CO_2: implications from the plant to the global-scale. *Plant Cell Environ.* **18**, 1214–1255 (1995).
13. Karnosky, D. F. *et al.* Scaling ozone responses of forest trees to the ecosystem level in a changing climate. *Plant Cell Environ.* **28**, 965–981 (2005).
14. Volk M. . *et al.* Grassland yield declined by a quarter in 5 years of free-air ozone fumigation. *Glob. Change Biol.* **12**, 74–83, doi:10.1111/j.1365-2486.2005.01083.x (2006).
15. Percy, K. E. *et al.* New exposure-based metric approach for evaluating O_3 risk to North American aspen forests. *Environ. Pollut.* **147**, 554–566 (2007).
16. Pleijel, H. *et al.* Relationships between ozone exposure and yield loss in European wheat and potato — a comparison of concentration- and flux-based exposure indices. *Atmos. Environ.* **38**, 2259–2269 (2004).
17. Essery, R. L. H., Best, M. J., Betts, R. A., Cox, P. M. & Taylor, C. M. Explicit representation of sub-grid heterogeneity in a GCM land-surface scheme. *J. Hydrometeorol.* **4**, 530–543 (2001).
18. Cox, P. M. *et al.* The impact of new GCM land-surface physics on the GCM simulation of climate and climate sensitivity. *Clim. Dyn.* **15**, 183–203 (1999).
19. Sanderson, M. G., Jones, C. D., Collins, W. J., Johnson, C. E. & Derwent, R. G. Effect of climate change on isoprene emissions and surface ozone levels. *Geophys. Res. Lett.* **30**, 1936, doi:10.1029/2003GL017642 (2003).
20. Karlsson, P. E. *et al.* New critical levels for ozone effects on young trees based on AOT40 and simulated cumulative leaf uptake of ozone. *Atmos. Environ.* **38**, 2283–2294 (2004).
21. New, M., Hulme, M. & Jones, P. Representing twentieth-century space-time climate variability. Part II. Development of 1901–96 monthly grids of terrestrial surface climate. *J. Clim.* **13**, 2217–2238 (2000).
22. Denman, K. L. *et al.* in *Climate Change 2007: The Physical Science Basis* (eds Solomon, S. *et al.*) 499–587 (Cambridge Univ. Press, Cambridge, UK, 2007).
23. Imhoff, M. L. *et al.* Global patterns in human consumption of net primary production. *Nature* **429**, 870–873 (2004).
24. Schröter, D. *et al.* Ecosystem service supply and vulnerability to global change in Europe. *Science* **310**, 1333–1337, doi:10.1126/science.1115233 (2005).
25. Nussbaum, S. & Fuhrer, J. Difference in ozone uptake in grassland species between open-top chambers and ambient air. *Environ. Pollut.* **109**, 463–471 (2000).
26. Sabine, C. L. *et al.* The oceanic sink for anthropogenic CO_2. *Science* **305**, 367–371 (2004).
27. Berntsen, T. K., Myhre, G., Stordal, F. & Isaksen, I. S. A. Time evolution of tropospheric ozone and its radiative forcing. *J. Geophys. Res.* **105**, 8915–8930 (2000).
28. Ramaswamy, V. *et al.* in *Climate Change 2001: The Scientific Basis* (eds Houghton, J. T. *et al.*) 350–416 (Cambridge Univ. Press, Cambridge, UK, 2001).

METHODS

Modelling ozone effect in MOSES-TRIFFID. Our approach is to modify net photosynthesis, A_p, by an 'uptake of O_3 factor', F:

$$A = A_p F \qquad (1)$$

From ref. 16,

$$F = 1 - a\,UO_{>FO3crit} \qquad (2)$$

where F represents the fractional reduction of plant production, $UO_{>FO3crit}$ is the instantaneous leaf uptake of O_3 over a plant type specific threshold, F_{O3crit}, in $nmol\,m^{-2}\,s^{-1}$. The fractional reduction of photosynthesis with O_3 uptake by leaves is represented by the plant type specific parameter, a (see Supplementary Table 1).

$$UO_{>FO3crit} = \max[(F_{O3} - F_{O3crit}), 0.0] \qquad (3)$$

From equations (2) and (3),

$$F = 1 - a\,\max[F_{O3} - F_{O3crit}, 0.0] \qquad (4)$$

F is dependent on the O_3 uptake rate by stomata over a critical (vegetation-dependent) threshold for damage. As an analogy of Ohm's law, the flux of O_3 to stomata, F_{O3} ($nmol\,O_3\,m^{-2}\,s^{-1}$), is given by,

$$F_{O3} = \frac{[O_3]}{R_a + \left[\frac{\kappa_{O3}}{g_l}\right]} \qquad (5)$$

where $[O_3]$ is the molar concentration of O_3 at reference level ($nmol\,m^{-3}$), R_a is the aerodynamic and boundary layer resistance between leaf surface and reference level ($s\,m^{-1}$), g_l is the leaf conductance for H_2O ($m\,s^{-1}$), and $\kappa_{O3} = 1.67$ is the ratio of leaf resistance for O_3 to leaf resistance for water vapour. The uptake flux is dependent on the stomatal conductance, which is dependent on the photosynthetic rate in MOSES. Given that g_l is a linear function of photosynthetic rate, A, (equation (13) in ref. 18), from equation (1) it follows,

$$g_l = g_p F \qquad (6)$$

where g_p is the leaf conductance in the absence of O_3 effects. The set of equations (4), (5) and (6) produces a quadratic in F that can be solved analytically.

To calibrate the ozone model, MOSES is first run from 1901 to 2002 assuming zero tropospheric ozone concentrations, and an initial pre-industrial equilibrium state. Year 2002 is repeated with geographically explicit tropospheric $[O_3]$ for 2002 from STOCHEM, using a first estimate of values for parameter a. Simulated half-hourly estimates of net primary productivity, NPP, and uptake of ozone, UO, are summed over the year. Relative annual yield, NPP/NPP_p (where NPP_p is the simulated NPP in the absence of plant ozone effects), is plotted against the cumulative annual uptake of ozone. The linear regression is compared with those derived from field observation[16,20]. Values of parameter a are adjusted, and the procedure repeated until the linear regression through the simulation points replicates that obtained from field studies[16,20] (Supplementary Fig. 2).

Data from field observation[16,20] are used to calibrate plant-ozone effects for the five plant functional types (PFTs) described by MOSES: broadleaved trees, conifers, C_3 grasses, C_4 grasses and shrubs. A 'high' and 'low' parameterization is chosen for each PFT to represent species sensitive and less sensitive, respectively, to ozone effects. In the absence of data, the 'low' conifer parameterization is assumed to be 3.8 times less sensitive than the high parameterization (corresponding to the same ratio for the broadleaved trees).

These sensitivity parameters are typically based on the response of young trees to ozone exposure[20] mainly from open-top chamber experiments (OTC). In some climatic conditions (high radiation and temperature), the microclimate conditions in OTC may differ from ambient air[25]. In the absence of observational data on plant-ozone uptake and ozone-induced yield reductions of trees in other life stages, we assume the response of young trees to be representative of all ages, and assume a constant ozone flux response of all plants throughout the growing period. The latter assumption may lead to an overestimate in the response of grasses to elevated ozone, as crops are known to exhibit variable flux response through the growing period. Threshold values, F_{O3crit}, are taken at 1.6 and $5\,nmol\,m^{-2}\,s^{-1}$ for the woody and grass PFTs, respectively. Although a threshold of $5\,nmol\,m^{-2}\,s^{-1}$ implies a smaller O_3 dose for grasses, the gradient of the dose–response function, a, is larger, and therefore grasses may become more sensitive to ozone exposure than trees at high ozone concentrations. For shrubs we assume the same plant-ozone sensitivity as broadleaf trees. We prescribe some agricultural lands, fixed at present-day coverage throughout the simulations, in which grasslands are assumed to be dominant.

Future tropospheric ozone concentrations. The Met Office's lagrangian tropospheric chemistry model STOCHEM[19] was used to generate monthly mean surface ozone concentrations for the present day (2000) using emissions from the IIASA CLE scenario[29], and for the future (2100) using emissions from the SRES A2 scenario.

Ozone levels for the pre-industrial period were also generated with this model[4]. Deposition fluxes of ozone and other trace gases were calculated using the stability of the boundary layer and fixed surface resistance values for land, sea and ice for each species. Biomass burning emissions were calculated using carbon emission data from ref. 30. The simulated surface ozone increases between 1900 and 2000 are mainly due to increased emissions of NO_x, but there have also been significant contributions from increases in hydrocarbon emissions associated with industrial activity in the northern mid-latitudes, and increasing biomass burning in the tropics.

The SRES A2 scenario for 2100 was chosen as this was the standard scenario used in the OxComp study presented in Chapter 4 of the IPCC Third Assessment Report[10], although now we consider this to be a pessimistic scenario. Like all the SRES scenarios it assumes no emission control measures, and thus may be considered as an upper limit. The largest increases in future emissions predicted under A2 are from industrialization in India and China, along with population growth in the tropics.

For the future simulation the effect of climate change over land was to slightly decrease ozone concentrations by about 2 p.p.b. (ref. 29), except over polluted areas. This run did not have interactive isoprene, nor soil NO_x, which might be expected to increase surface ozone in a 2100 climate.

For each simulation (pre-industrial, present day and future), STOCHEM was integrated for 5 years and 4 months. For each calendar month, the average of the last five years of the run was calculated. Thus for each simulation 12 monthly fields of diurnal mean O_3 concentrations were generated. Values for intermediate years between those simulated were generated by linear interpolation for the appropriate month.

29. Dentener, F. D. *et al.* The global atmospheric environment for the next generation. *Environ. Sci. Technol.* **40**, 3586–3594 (2005).
30. van der Werf, G. R., Randerson, J. T., Collatz, G. J. & Giglio, L. Carbon emissions from fires in tropical and subtropical ecosystems. *Glob. Change Biol.* **9**, 547–562 (2003).